Title
Transport gap in SmB6 protected against disorder

Journal
Proceedings of the National Academy of Sciences of the United States of America, 116(26)

ISSN
0027-8424

Authors
Eo, Yun Suk
Rakoski, Alexa
Lucien, Juniar
et al.

Publication Date
2019-06-25

DOI
10.1073/pnas.1901245116

Peer reviewed

Transport gap in SmB_6 protected against disorder

Yun Suk Eo[a,1], Alexa Rakoski[a], Juniar Lucien[a], Dmitri Mihaliov[a], Çağlıyan Kurdak[a], Priscila F. S. Rosa[b], and Zachary Fisk[c,1]

[a]Department of Physics, University of Michigan, Ann Arbor, MI 48109-1040; [b]Los Alamos National Laboratory, Los Alamos, NM 87545; and [c]Department of Physics and Astronomy, University of California, Irvine, CA 92697

Contributed by Zachary Fisk, April 29, 2019 (sent for review January 23, 2019; reviewed by Piers Coleman and Gilbert George Lonzarich)

The inverted resistance method was used in this study to extend the bulk resistivity of SmB_6 to a regime where the surface conduction overwhelms the bulk. Remarkably, regardless of the large off-stoichiometric growth conditions (inducing disorder by samarium vacancies, boron interstitials, etc.), the bulk resistivity shows an intrinsic thermally activated behavior that changes ∼7–10 orders of magnitude, suggesting that SmB_6 is an ideal insulator that is immune to disorder.

topological insulator | heavy-fermion materials | semiconductors

Transport experiments on the archetypic Kondo insulator SmB_6 have shown that the low-temperature plateau in its electrical resistivity is due to a surface conducting state which develops below 4 K (1–7), a finding consistent with the theoretical suggestion of topological insulating character (8, 9) but one which remains a matter of contention. Our purpose here is not to review the extensive and in many aspects perplexing experimental record, but to present additional Corbino disk-based transport data able to separate effectively the bulk and surface contributions. We find that there are no bulk in-gap states that can contribute to dc transport in stoichiometric flux-grown SmB_6 crystals: the bulk dc resistivity rises by a factor of 10^{10} on cooling from 300 K to 2 K. We suggest that this gap protection is the defining characteristic of such materials.

A further key aspect to be considered in SmB_6 is the role of disorder. Conventional narrow-band semiconductors respond to disorder in electrical transport by the formation of in-gap impurity states. Remarkably, we find that disorder (e.g., defects such as samarium vacancies and boron interstitials) induced by the growth does not influence the bulk activated behavior of SmB_6. There are very few cases where the gap is not compromised by defects such as the BCS gap in superconductors (10). In most band-gapped materials, disorder plays a significant role. Our measurements show a thermally activated behavior with an activated gap of about 4 meV for all measured samples, as summarized in Table 1.

Results

To study the bulk transport in the presence of surface conduction, we use the recently developed inverted resistance measurement (11). This method allows us to measure bulk resistivity in the dc limit even in the regime in which surface conduction dominates. It is important to note that in the presence of both surface and bulk conduction, the resistance ratio (i.e., R_{2K}/R_{300K}) from conventional four-contact measurements is neither the bulk resistivity ratio nor the surface resistivity ratio (11). In *SI Appendix*, section A, we demonstrate the substantial difference between a typical four-contact measurement in an unpolished sample and our Corbino disk measurement to demonstrate this point.

We illustrate our transport geometry and the measurement configuration. Our transport geometry design of the top, side, and bottom is shown in Fig. 1 *A*–*C*, respectively. We also show photographs of one of the actual samples, identical to this design, in Fig. 1 *D* (top), *E* (side), and *F* (bottom). A four-terminal Corbino disk can be measured by $R_{1,4;2,3}$ $(=V_{2,3}/I_{1,4})$, which can be regarded as a standard resistance measurement (R_{Std}). If the change in surface resistivity (ρ_s (Ω)) with temperature is not strong compared with the bulk resistivity (ρ_b ($\Omega\cdot$cm)), the standard two-channel model is a good approximation that works well for R_{Std} in the full temperature range,

$$R_{\mathrm{Std}} = C_0(\rho_s^{-1} + \gamma\rho_b^{-1})^{-1}, \quad [1]$$

where the geometric prefactor C_0 is $\ln(r_{\mathrm{out}}/r_{\mathrm{in}})/2\pi$ for a Corbino disk, and γ is the effective thickness that asymptotically approaches t (true thickness) when the sample is very thin, but is independent of t when the sample is very thick (11).

In the surface-dominated regime, below about 4 K, the inverted resistance (R_{Inv}) can be measured by either $R_{1,4;5,6}$ or $R_{1,2;3,4}$. The key idea is that the Corbino disk is used to enclose the current flowing on the surface, and the voltage leads are on a surface region exterior to that disk. Then, since the main surface current path is blocked, the voltage drop can exist only from a current that includes the bulk path. We show that this idea of the inverted resistance measurement can be illustrated by a simple resistor circuit as shown in Fig. 1*G*. The resistors that represent the surface path are shown in blue and the resistor that represents the bulk path is shown in red. The majority of the surface current flows from 1 to 4. In addition, a small current flows through 1→5→6→4. The voltage measured between 5 and 6 is then

$$V = I_{tot} \times \left(\frac{R^s_{top}}{R^b + R^s_{bott} + R^s_{side} + R^s_{top}}\right) \times R^s_{bott}, \quad [2]$$

where I_{tot} is the total current flowing through the circuit. We can assume the resistors that represent the surface (blue resistors) are proportional to ρ_s, and the bulk (red resistor) are proportional to

Significance

The realization of modern electrical and optoelectrical devices is possible because of the successful control of point defects in semiconductors or narrow band-gapped insulators. Recently, a new subclass of these semiconductors has been discovered, so-called topological insulators (TIs). These 3D TIs harbor a unique 2D conduction layer on the surfaces that can be potentially applicable for novel quantum devices. The access of these surface states, however, is easily hindered by bulk conduction from unintentional defects. Surprisingly, by using a unique resistance measurement in a strongly correlated TI SmB_6, we find that typical defect signatures of a semiconductor in electrical transport are absent in the SmB_6 bulk, including samples prepared with large samarium-to-boron off-stoichiometry.

Author contributions: Y.S.E., Ç.K., and P.F.S.R. designed research; P.F.S.R. contributed new reagents/analytic tools; Y.S.E., A.R., J.L., D.M., Ç.K., and P.F.S.R. performed research; Y.S.E., A.R., J.L., D.M., Ç.K., and P.F.S.R. analyzed data; and Y.S.E., Ç.K., P.F.S.R., and Z.F. wrote the paper.

Reviewers: P.C., Rutgers University; and G.G.L., University of Cambridge.

The authors declare no conflict of interest.

[1]To whom correspondence may be addressed. Email: eohyung@umich.edu or zfisk@uci.edu.

This article contains supporting information online at www.pnas.org/lookup/suppl/doi:10.1073/pnas.1901245116/-/DCSupplemental.

Published online June 10, 2019.

Table 1. Summary of our results

Sample	r	E_a, meV	ρ_s, kΩ	Hardness, kgf/mm^2
S1	0	4.01 ± 0.0054	3.1	2,191 ± 125
S2	0.1	4.12 ± 0.0041	1.6	1,913 ± 16.5
S3	0.25	3.97 ± 0.0047	1.5	1,781 ± 111
S4	0.40	3.85 ± 0.0038	2.8	1,563 ± 50.8

Samples were grown with starting composition Sm:B:Al = $(1 - r)$:6:700, where r is the percentage of Sm vacancies. Detailed information of crystal characterization, including X-ray, Auger, and hardness measurements, can be found in *SI Appendix*, section B.

ρ_b. The inverted resistance below the bulk-to-surface crossover temperature, in the $\rho^b/\rho^s t \to \infty$ limit, follows as

$$R_{\mathrm{Inv}} = C_1 t \frac{\rho_s^2}{\rho_b}, \qquad [3]$$

where C_1 is a geometric prefactor for the inverted resistance. We note that this functional form is equivalent to the more general approach using series expansion of the scaling argument that was shown in ref. 11. In *SI Appendix*, section C, we briefly review this scaling argument and a more detailed explanation of the circuit model in Fig. 1*G*. The corresponding γ and C_1 are found from finite-element analysis, similar to the derivation of bulk resistivity extraction in ref. 11.

We now discuss our experimental results beginning with our stoichiometrically grown sample (S1). Fig. 2*A* shows the measured resistance (R_{Std} [blue] and R_{Inv} [red]) from sample S1. The qualitative behavior in Fig. 2*A* is consistent with what we expect when the bulk resistivity is governed intrinsically, $\rho_b \propto \exp(E_a/k_B T)$, where E_a is the activation energy. In the high-temperature regime, above ∼4 K, both R_{Std} and R_{Inv} increase when the temperature is lowered, consistent with Eq. **1** in the bulk-dominated regime ($\rho_b/\rho_s t \to \infty$). Below ∼4 K, R_{Std} develops a plateau which corresponds to a sheet resistance of ρ_s = 3 kΩ according to Eq. **1** in the surface-dominated regime ($\rho_b/\rho_s t \to 0$). R_{Inv}, on the other hand, drops as the temperature is lowered. This is consistent with Eq. **3** when the bulk resistivity follows $\rho_b \propto \exp(E_a/k_B T)$. Below 2 K, the inverted resistance becomes too small, and the measurement is limited by the amplifier performance. Here, we present only the data that are meaningful, above this performance limit.

Next, we consider the nonstoichiometrically grown SmB_6 samples. We present the results of sample S4 in Fig. 2*B*. In the bulk-dominated regime, above ∼4 K, the temperature response of the resistances of all samples behaved qualitatively identically to sample S1 results. In the surface-dominated regime, below ∼4 K, R_{Std} shows a plateau that corresponds to a ρ_s in the 1- to 3-kΩ range. In contrast, R_{Inv} in the surface-dominated regime drops at first, consistent with Eq. **3** when the bulk resistivity keeps rising. Below ∼2.5 K, however, the resistance becomes less temperature dependent. The magnitude of this resistance plateau is lower for samples that are grown with less Sm.

Discussion

The conversion to bulk resistivity (ρ_b) from the measured resistances can be found using Eqs. **1** and **3** with the coefficients found numerically. We present more details of this conversion in *SI Appendix*, section D. The bulk resistivities converted from the resistance measurements are shown in Fig. 3. Sample S1 (shown in black) shows a thermally activated exponential behavior (E_a = 4.01 meV) that changes by ∼10 orders of magnitude. The resistivity shows an intrinsic semiconductor behavior in the full temperature range, without any signs of the saturation regime of an extrinsic semiconductor or variable range hopping. Below 0.4 K^{-1} (or above ∼2.5 K), the nonstoichiometrically grown SmB_6 samples (samples S2, S3, and S4) show almost identical activation energies, and the resistivity rises at least 7 orders of magnitude.

It is well known from previous Hall measurements that the bulk resistivity rise of SmB_6 is due to the thermally activated bulk carriers (12–16). In our stoichiometrically grown sample (sample S1) result, the activated behavior continues at low temperatures, indicating that the carrier density continues to decrease as the temperature is decreased with a total of ∼10 orders of magnitude. From this continuing exponential decrease, we estimate a carrier density of 10^{12} (1/cm^3) at the lowest measurable temperature (2 K). This implies that there are only ∼10^7 carriers in the bulk region of our entire sample at this temperature, and there would be less than 1 bulk carrier below 1 K by extrapolating the thermally activated behavior. The off-stoichiometrically grown samples (samples S2, S3, and S4) also indicate that no more than 10^{15} (1/cm^3) bulk carriers are left before the bulk resistivity saturates below 2.5 K. For the saturation of the nonstoichiometrically grown samples, the magnitudes are too high for them to be attributed to the extrinsic regime of a semiconductor. It is important to note that this is in stark contrast to other hexaboride systems and other Kondo insulators that all show strong dependence of disorder in the temperature-dependent resistivity measurements (*SI Appendix*, section F and Tables S2 and S3). This result is also promising when comparing to the bulk of other 3D topological insulators (TIs), in which purifying bulk is an ongoing challenge (17, 18).

Nevertheless, the low-temperature resistivity saturations in the nonstoichiometrically grown samples indicate that there is a small response to disorder. Fits of the data to the temperature-dependent hopping conduction through an impurity band are not compelling (*SI Appendix*, section F), and the high resistivity magnitude makes this case unlikely. One possibility is that the conduction path has a confined or lower-dimensional percolative current channel instead of a homogeneous channel in the bulk. A plausible possibility is that extended defects, such as grain boundaries and threading dislocations, harbor topologically protected conduction and may be a conduction path. We observe signatures of twinning in our samples and a smaller hardness in the off-stoichiometric–grown samples that

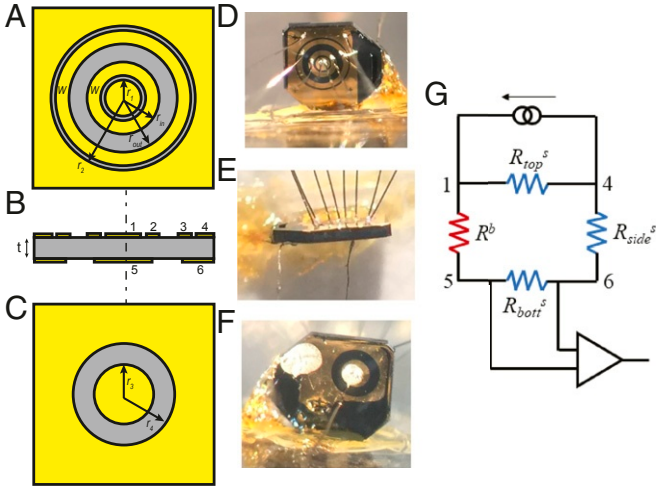

Fig. 1. Schematic diagram and actual image of the transport geometry used in this experiment. (*A–C*) Schematic diagram of (*A*) top surface, (*B*) side surface, and (*C*) bottom surface. (*D–F*) Actual image of the (*D*) top surface, (*E*) side surface, and (*F*) bottom surface. The dimensions are r_1 = 100 μm, r_2 = 800 μm, r_{in} = 200 μm, r_{out} = 300 μm, W = 75 μm, r_3 = 165 μm, and r_4 = 290 μm. (*G*) The equivalent circuit model of the inverted resistance measurement ($R_{1,4;5,6}$) at very low temperatures where the transport is dominated by surface conduction.

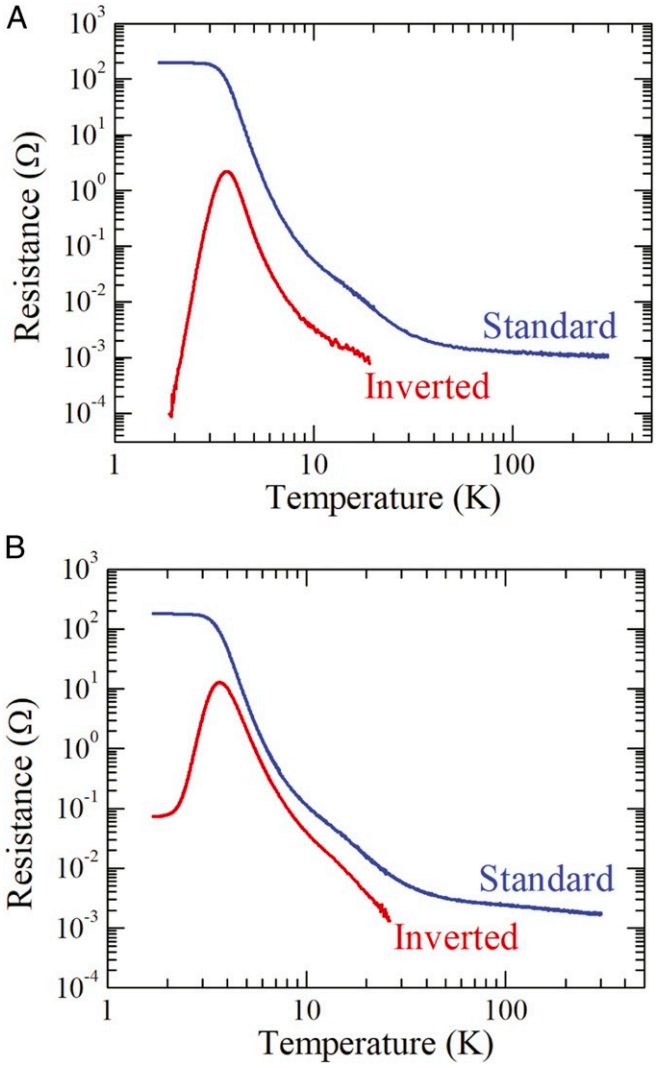

Fig. 2. Resistance of the standard and inverted resistance measurements. (*A*) Results for the stoichiometrically grown SmB_6 (sample S1). (*B*) Results from sample S4.

indicate that crystallographic defects are certainly present in the samples we measure. So far, there seems to be only theory work on topologically protected extended defect conduction for weak 3D TIs (19) and higher-order topological insulators (20).

To the best of our knowledge, our findings of the robust intrinsic insulating behavior and the high bulk resistivity plateau in the nonstoichiometrically grown samples can be explained neither by the standard theory of disorder in semiconductors nor by the previously established framework of Kondo insulators with disorder. We note that the immunity of disorder seems present only in electrical transport in the dc limit. Previous experiments, including specific heat and neutron scattering (21), Raman spectroscopy (22), thermal transport (23), and ac conductivity in the terahertz range (24), report that impurities (defects) and disorder may play a significant role in the bulk of SmB_6. This is not, however, necessarily in contradiction with our findings. Recent electron spin resonance measurements in SmB_6 with Gd^{3+} impurities show that the Gd ions are locally surrounded by metallic puddles.* Further, recent scanning tunneling spectroscopy measurements show that the surface states of SmB_6 are only locally destroyed by magnetic impurities (25). In light of these recent experiments, we propose that the insulating bulk of SmB_6 may treat impurities as vacuum and, as a result, screen these impurities in a way that electrical transport in the dc limit is immune to them. Within this framework, the bulk resistivity plateaus observed in the nonstoichiometric samples might be a result of the percolation of these metallic puddles at higher concentrations.

Finally, we note that several theory works have revisited the bulk gap of SmB_6, motivated by the recent bulk-like quantum oscillations (26). A scenario for disorder in the bulk has been recently proposed by Shen et al. (27). The authors propose a two-band model within the non-Hermitian formalism in the presence of disorder. This leads to states from the conduction and valence band spilling into the gap. Under certain conditions of disorder and gap, the authors find that quantum oscillations can exist with a frequency consistent with that of the unhybridized bands instead of an existence of a neutral Fermi surface. Shortly after, Harrison (28) used this formalism in the limit of strong disorder and found that the band gap may close completely, leading to the formation of a nodal semimetal. Harrison (28) predicts that there should be a linear temperature dependence in bulk conductivity if there is a saturation behavior coming from the

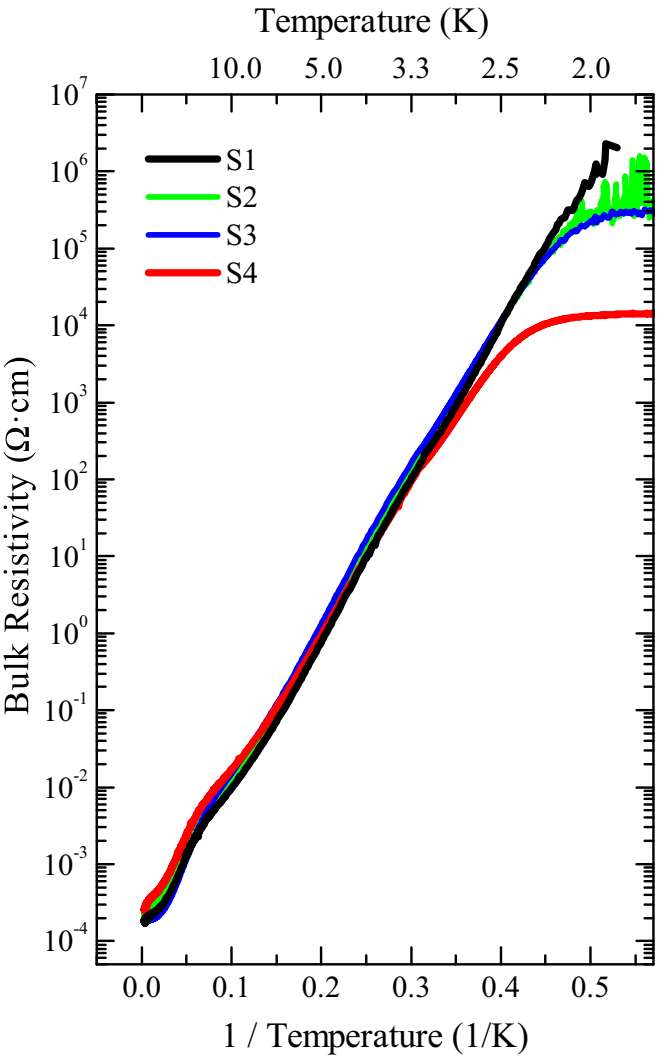

Fig. 3. Bulk resistivity conversion of the stoichiometrically grown (S1) and nonstoichiometrically grown (S2, S3, and S4) SmB_6 samples.

*J. Souza *et al.*, "Electron spin resonance in Gd^{3+} doped Kondo insulator SmB_6" in *International Conference on Magnetism 2018*, San Francisco (2018).

bulk. Our data, however, show that the saturation regime does not follow any power of temperature (*SI Appendix*, section F). In the weak disorder case, where a gap remains without a node, the states filled in the gap are likely localized states. Electrical transport in the dc limit seems yet elusive for those localized states and may require future theoretical studies.

There are also recent theory works that revisit the bulk gap formation at a more fundamental level (29–34). For example, Chowdhury et al. (34) suggest that, in the limit of large Coulomb interactions between the f- and d-electrons, the Hamiltonian can be expressed in terms of a spinon and a fermionic composite exciton, formed by a d-electron and a holon. These composite excitons and spinons hybridize and form a chargeless gap, but the Fermi energy can still cross those chargeless bands. Alternatively, Baskaran (32) and Erten et al. (33) revisit the possibility that Kondo insulators can be viewed as a neutral Majorana Fermi sea. Erten et al. (33) note that gauge invariance has to be broken for the quasi-particle to couple with only the magnetic field and not the electric field. Erten et al. (33) suggest that SmB_6 may have a topologically unstable order parameter that fails to be a superconductor, but instead may be in an insulating ground state. In this context, disorder may introduce competing dielectric phases. The diversity of theoretical models mentioned above is remarkable, and we believe our experimental results on flux-grown SmB_6 will guide further theoretical progress.

Conclusion

The bulk transport of stoichiometrically and nonstoichiometrically grown SmB_6 samples, grown by a flux method, was studied using the inverted resistance measurement. Using the double-sided Corbino disk geometry, stoichiometrically grown SmB_6 shows a robust thermally activated bulk resistivity rise. The nonstoichiometrically grown SmB_6 samples, grown with substantially less samarium, show an almost identical thermally activated behavior until a bulk resistivity plateau develops. Our results suggest that the bulk of SmB_6 is immune to disorder originating from point defects such as samarium vacancies and interstitial boron impurities. The robust insulating bulk in SmB_6 may be important for applications in which high purification is necessary. For example, in spintronics applications of 3D TIs, there would be no parallel conduction channel from the bulk. For topological quantum computers, we expect the Majorana modes to be well defined because the lifetime of the Majorana modes will not be limited by the bulk channel.

Materials and Methods

Single crystalline samples were grown by the Al-flux technique. The mixture of samarium pieces (Ames Laboratory; 99.99%), boron powder (99.99%) and aluminum shots (99.999%) was placed in an alumina crucible and loaded in a vertical tube furnace with Ar flow (99.999%). Samples were synthesized with starting compositions Sm:B:Al = $(1 - r)$:6:700, where r is the nominal composition ratio of the vacancies, ranging from 0 to 0.40. We expect sample S1 in which r = 0 to be stoichiometric, whereas the other samples are expected to have a higher disorder level. X-ray and Auger electron spectroscopy measurements could not unambiguously determine point defect levels, but we do see differences that indicate the overall physical properties are changing from hardness measurements (Table 1). A detailed description is presented in *SI Appendix*, section B.

For preparing the transport geometry, the samples were fine polished with a final step of aluminum oxide slurry that has a particle size of 0.3 μm. The Corbino-disk patterns were fabricated using photolithography, followed by e-beam evaporation of Ti/Au (20 Å/1500 Å). We used a home-built instrumentation amplifier in addition to an external lock-in amplifier in the Dynacool PPMS for measurement.

ACKNOWLEDGMENTS. We thank J. W. Allen, K. Sun, and J. Denlinger for useful discussions and advice on improving the manuscript. Y.S.E. is thankful to J. Paglione, M. S. Fuhrer, W. T. Fuhrman, N. P. Butch, and S. H. Lee for discussions of this work. We also thank B. L. Scott for the discussion of the single-crystal X-ray diffraction data and Zhongrui (Jerry) Li for assistance with the Auger electron spectroscopy experiments. Funding for this work was provided by NSF Grants DMR-1441965, DMR-1643145, and DGE-1256260. The authors acknowledge the University of Michigan College of Engineering for financial support and the Michigan Center for Materials Characterization for use of the instruments and staff assistance. P.F.S.R. acknowledges support from the Laboratory Directed Research and Development program of Los Alamos National Laboratory under Project 20160085DR.

1. S. Wolgast *et al.*, Low-temperature surface conduction in the Kondo insulator SmB_6. *Phys. Rev. B* **88**, 180405(R) (2013).
2. D. Kim *et al.*, Surface Hall effect and nonlocal transport in SmB_6: Evidence for surface conduction. *Sci. Rep.* **3**, 3150 (2013).
3. S. Wolgast *et al.*, Magnetotransport measurements of the surface states of samarium hexaboride using Corbino structures. *Phys. Rev. B* **92**, 115110 (2015).
4. Y. Nakajima, P. Syers, X. Wang, R. Wang, J. Paglione, One-dimensional edge state transport in a topological Kondo insulator. *Nat. Phys.* **12**, 213–217 (2016).
5. P. Syers, D. Kim, M. Fuhrer, J. Paglione, Tuning bulk and surface conduction in the proposed topological Kondo insulator SmB_6. *Phys. Rev. Lett.* **114**, 096601 (2015).
6. S. Thomas *et al.*, Weak antilocalization and linear magnetoresistance in the surface state of SmB_6. *Phys. Rev. B* **94**, 205114 (2016).
7. N. Wakeham, Y. Wang, Z. Fisk, F. Ronning, J. Thompson, Surface state reconstruction in ion-damaged SmB_6. *Phys. Rev. B* **91**, 085107 (2015).
8. M. Dzero, K. Sun, V. Galitski, P. Coleman, Topological Kondo insulators. *Phys. Rev. Lett.* **104**, 106408 (2010).
9. T. Takimoto, SmB_6: A promising candidate for a topological insulator. *J. Phys. Soc. Jpn.* **80**, 123710 (2011).
10. P. Anderson, Theory of dirty superconductors. *J. Phys. Chem. Sol.* **11**, 26–30 (1959).
11. Y. Eo, K. Sun, C. Kurdak, D. Kim, Z. Fisk, Inverted resistance measurements as a method for characterizing the bulk and surface conductivities of three-dimensional topological insulators. *Phys. Rev. Appl.* **9**, 044006 (2018).
12. J. Allen, B. Batlogg, P. Wachter, Large low-temperature Hall effect and resistivity in mixed-valent SmB_6. *Phys. Rev. B* **20**, 4807 (1979).
13. S. Molnar *et al.*, Study of the energy gap in single crystal SmB_6. *Valence Instabilities: Proceedings of the International Conference Held in Zürich, Switzerland, April 13–16* (North Holland, Amsterdam, 1982), p. 389.
14. T. Kasuya *et al.*, Mechanisms for anomalous properties in SmB_6. *J. Magn. Magn. Mater.* **31-34**, 447–450 (1983).
15. N. Sluchanko *et al.*, Nature of the low-temperature anomalies in the physical properties of the intermediate-valent compound SmB6. *J. Exp. Theor. Phys.* **88**, 533–537 (1999).
16. N. Sluchanko *et al.*, Intragap states in SmB_6. *Phys. Rev. B* **61**, 9906–9909 (2000).
17. Y. Ando, Topological insulator materials. *J. Phys. Soc. Jpn.* **82**, 102001 (2013).
18. M. Brahlek, N. Koirala, N. Bansal, S. Oh, Transport properties of topological insulators: Band bending, bulk metal-to-insulator transition, and weak anti-localization. *Solid State Commun.* **215-216**, 54–62 (2015).
19. R. Ying, Y. Zhang, A. Vishwanath, One-dimensional topologically protected modes in topological insulators with lattice dislocations. *Nat. Phys.* **5**, 298–303 (2009).
20. R. Queiroz, I.-C. Fulga, N. Avraham, H. Beidenkopf, J. Cano, Partial lattice defects in higher order topological insulators. arXiv:1809.03518 (10 September 2018).
21. W. Fuhrman *et al.*, Screened moments and extrinsic in-gap states in samarium hexaboride. *Nat. Commun.* **9**, 1539 (2018).
22. M. Valentine *et al.*, Breakdown of the Kondo insulating state in SmB_6 by introducing Sm vacancies. *Phys. Rev. B* **94**, 075102 (2016).
23. M. Boulanger *et al.*, Field-dependent heat transport in the Kondo insulator SmB_6: Phonons scattered by magnetic impurities. *Phys. Rev. B* **97**, 245141 (2018).
24. N. Laurita *et al.*, Anomalous three-dimensional bulk ac conduction within the Kondo gap of SmB_6 single crystals. *Phys. Rev. B* **94**, 165154 (2016).
25. L. Jiao *et al.*, Magnetic and defect probes of the SmB_6 surface state. *Sci. Adv.* **4**, eaau4886 (2018).
26. B. Tan *et al.*, Unconventional Fermi surface in an insulating state. *Science* **349**, aaa7974 (2015).
27. H. Shen, B. Zhen, L. Fu, Topological band theory for non-Hermitian Hamiltonians. *Phys. Rev. Lett.* **120**, 146402 (2018).
28. N. Harrison, Highly asymmetric nodal semimetal in bulk SmB_6. *Phys. Rev. Lett.* **121**, 026602 (2018).
29. O. Erten, P. Ghaemi, P. Coleman, Kondo breakdown and quantum oscillations in SmB6. *Phys. Rev. Lett.* **116**, 046403 (2016).
30. L. Zhang, X. Song, F. Wang, Quantum oscillation in narrow-gap topological insulators. *Phys. Rev. Lett.* **116**, 046404 (2016).
31. J. Knolle, N. Cooper, Excitons in topological Kondo insulators: Theory of thermodynamic and transport anomalies in SmB_6. *Phys. Rev. Lett.* **118**, 096604 (2017).
32. G. Baskaran, Majorana Fermi sea in insulating SmB_6: A proposal and a theory of quantum oscillations in Kondo insulators. arXiv:1507.03477v1 (13 July 2015).
33. O. Erten, P. Chang, P. Coleman, A. Tsvelik, Skyrme insulators: Insulators at the brink of superconductivity. *Phys. Rev. Lett.* **119**, 057603 (2017).
34. D. Chowdhury, I. Sodemann, T. Senthil, Mixed-valence insulators with neutral Fermi surfaces. *Nat. Commun.* **9**, 1766 (2018).